J. Phys. Chem. Solids Vol. 53, No. 7, pp. 935–939, 1992
Printed in Great Britain.

0022-3697/92 $5.00 + 0.00

DIELECTRIC STUDY OF $CH_3NH_3PbX_3$ (X = Cl, Br, I)†

NORIKO ONODA-YAMAMURO, TAKASUKE MATSUO and HIROSHI SUGA
Department of Chemistry and Microcalorimetry Research Center, Faculty of Science, Osaka University, Toyonaka, Osaka 560, Japan

(*Received* 4 *September* 1991; *accepted* 18 *December* 1991)

Abstract—Complex dielectric permittivities of $CH_3NH_3PbX_3$ (X = Cl, Br, I) were measured at frequencies between 20 Hz and 1 MHz and at temperatures between 20 and 300 K (15 and 350 K for the iodide). Discontinuities or a sharp bend of the real part of the dielectric permittivity occurred at the phase transitions, except at the tetragonal (*I*4/*mcm*)-cubic phase transition where the permittivity showed no apparent change. The dielectric behavior in the cubic and tetragonal (*I*4/*mcm*) phases are described well by a modified Kirkwood–Fröhlich equation. Dielectric dispersions were found in the orthorhombic phase of $CH_3NH_3PbBr_3$ and $CH_3NH_3PbI_3$ at temperatures between 30 and 120 K.

Keywords: Dielectric permittivity, relaxation time, methylammonium trihalogenoplumbate(II), phase transition, orientational disorder.

1. INTRODUCTION

$CH_3NH_3PbX_3$ (X = Cl, Br, I) crystallizes in the cubic perovskite structure in the highest temperature phases [1] and undergoes two or three phase transitions [2, 3]. Table 1 summarizes the transition temperatures determined by the present authors [4] and the space groups determined by Poglitsch and Weber [3]. The bromide has two tetragonal phases. One of them corresponds to the tetragonal phase of the chloride and the other to that of the iodide. Hereafter, we designate each phase as follows: cubic (cubic $Pm3m$), tetragonal I (tetragonal $I4/mcm$), tetragonal II (tetragonal $P4/mmm$), orthorhombic I (orthorhombic $P222_1$), and orthorhombic II (orthorhombic $Pna2_1$). A calorimetric study reported in our recent paper [4] showed that all the phase transitions were of the first order. The large transition entropies indicated that the phase transitions are of the order–disorder type. The entropy values were interpreted in terms of structural models in which $CH_3NH_3^+$ ions (abbreviated MA ion hereafter) are disordered with respect to the orientations of the C–N axis itself and around the C–N axis.

Molecular motion of the MA ion was investigated by ^1H, ^2H and ^{14}N NMR [2, 5–7]. In the cubic and tetragonal I phases, the MA ion undergoes extremely rapid overall reorientation [2, 5–7]. The reorientation of the C–N axis approaches the rapidity calculated for the free ion [5]. In the lower temperature phases (tetragonal II, orthorhombic I and II), the reorientation of the C–N axis seems to be frozen but that around the C–N axis persists [5]. A precessional motion of the C–N axis was suggested in the tetragonal II phase [6, 7].

In the present paper, we report the dielectric properties of $MAPbX_3$ at low temperatures. Since the MA ion has a permanent dipole moment, a dielectric study is a powerful technique by which to investigate the orientational motion. Dielectric measurements have already been carried out by Poglitsch and Weber [3] at frequencies of 50–150 GHz and temperatures of 100–300 K. They found a discontinuity in the dielectric constant at the orthorhombic–tetragonal phase transition for all three substances. A picosecond relaxation due to the dynamic disorder of the reorientating MA ion was revealed in the high-temperature phases. However, the dielectric behavior of the tetragonal II phase was not clear in their measurement because of its narrow temperature range. Since the comparatively large values ($18 \sim 30$) of ϵ' (the real part of the permittivity) at 100 K suggest that one should expect a further temperature dependence of ϵ' below 100 K, we extended the complex permittivity measurement to lower frequencies and lower temperatures.

2. EXPERIMENTAL

The samples were prepared in the same way as described in a previous paper [4]. The complex dielectric permittivity was measured by the two-terminal method using a precision LCR meter (Hewlett-Packard 4284A) in the frequency range from 20 Hz to 1 MHz at temperatures between 20 and 300 K (15 and 350 K for $MAPbI_3$). The details of the cryostat have been described elsewhere [8]. Powdered crystals were pressed to form disks, with a typical size

†Contribution No. 47 from the Microcalorimetry Research Center.

Table 1. Structures and transition temperatures of $CH_3NH_3PbX_3$ (X = Cl, Br, I)†

$CH_3NH_3PbCl_3$	orthorhombic	———	tetragonal	———		———	cubic
	$P222_1$	171.5 K	$P4/mmm$		177.2 K		$Pm3m$
$CH_3NH_3PbBr_3$	orthorhombic	———	tetragonal	———	tetragonal	———	cubic
	$Pna2_1$	148.8 K	$P4/mmm$	154.0 K	$L4/mcm$	236.3 K	$Pm3m$
$CH_3NH_3PbL_3$	orthorhombic	———		———	tetragonal	———	cubic
	$Pna2_1$		161.4 K		$L4/mcm$	330.4 K	$Pm3m$

† Space group from Poglitsch and Weber [3] and transition temperatures from Onoda-Yamamuro *et al.* [4]

13.05 mm in diameter and 0.818 mm in thickness (for $MAPbBr_3$). The mass density of the disk was 3.52 g cm^{-3}, as compared with the X-ray diffraction value 3.87 g cm^{-3} [3]. The disk was annealed at 350 K for about 1 h to remove the effect of the pressure applied. Gold was vapor-deposited on the circular surfaces of the disk as electrodes. The temperature of the sample was measured with a chromel–constantan thermocouple to an accuracy of ±0.2 K above 40 K. The accuracy below 40 K was ±0.3 K.

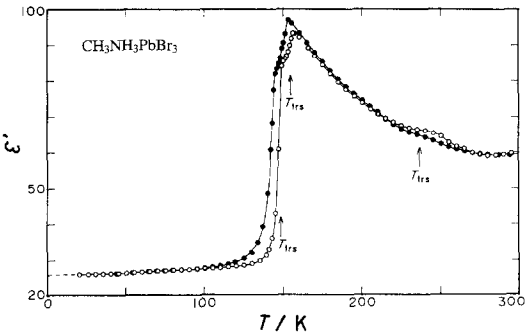

Fig. 2. Temperature dependence of the real part of the dielectric permittivity of $CH_3NH_3PbBr_3$ taken at 1 kHz in heating (open symbols) and cooling (closed symbols).

3. RESULTS AND DISCUSSION

The temperature dependence of the real part of the dielectric permittivity is shown in Figs 1–3 for $MAPbCl_3$, $MAPbBr_3$ and $MAPbI_3$, respectively. Since no frequency dependence was found except in the lowest temperature phases of $MAPbBr_3$ and $MAPbI_3$ (see below), only the 1 kHz data are shown. Symbols ● and ○ denote the data obtained on cooling and heating, respectively. Arrows in the figures indicate the transition temperatures determined by our heat capacity measurements [4]. In Fig. 2, the small hump around 240 K and the slight increase above 290 K where a decrease is expected are due to a small amount of water which was trapped in the sample disks or adsorbed on the sample surface and grain boundary. The values ϵ' and ϵ'' were frequency dependent in these temperature ranges and the effect of the water decreased in magnitude with increasing frequency.

With decreasing temperature, the ϵ' values of $MAPbCl_3$ increased with an increasing slope and dropped at the cubic–tetragonal II phase transition and further at the tetragonal II–orthorhombic I transition. For $MAPbBr_3$, the ϵ' values increased with decreasing temperature in the cubic and tetragonal I phases. No obvious change occurred at the transition between these two phases. A sharp bend and discontinuous decrease were observed at the tetragonal I–tetragonal II and the tetragonal II–orthorhombic II transitions, respectively. For $MAPbI_3$, the dielectric permittivity of the cubic phase continued without break onto that of the tetragonal

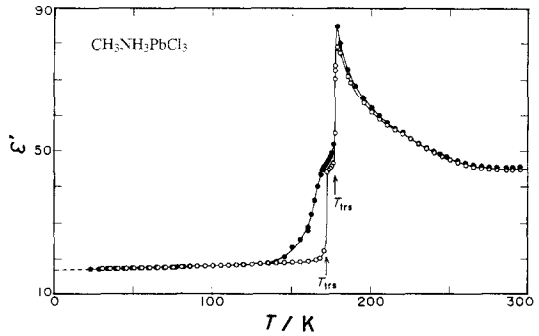

Fig. 1. Temperature dependence of the real part of the dielectric permittivity of $CH_3NH_3PbCl_3$ taken at 1 kHz in heating (open symbols) and cooling (closed symbols).

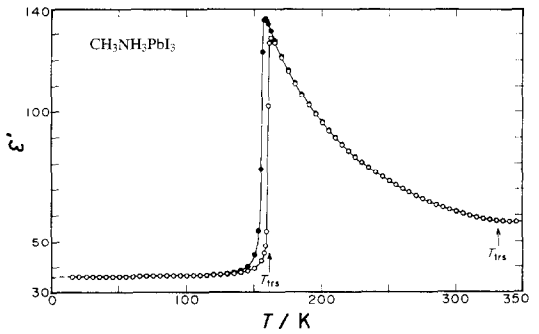

Fig. 3. Temperature dependence of the real part of the dielectric permittivity of $CH_3NH_3PbI_3$ taken at 1 kHz in heating (open symbols) and cooling (closed symbols).

II phase, following a Curie–Weiss type temperature dependence down to the transition temperature 161 K, where ϵ' showed a discontinuity at the tetragonal I–orthorhombic II transition.

Cubic and tetragonal I *phases*

In these phases, the ϵ' curves show a $1/T$ (or $1/(T - T_c)$)-like temperature dependence. This indicates that the dipoles are disordered in these phases. The static permittivity ϵ_0 of the pure polar liquid is described by the Kirkwood–Fröhlich equation [9],

$$\frac{(\epsilon_0 - \epsilon_\infty)(2\epsilon_0 + \epsilon_\infty)}{\epsilon_0(\epsilon_\infty + 2)^2} = \frac{1}{9\epsilon_v} g \frac{N\mu^2}{k_B T}, \qquad (1)$$

where ϵ_∞ denotes the permittivity at the high-frequency limit, ϵ_v the permittivity of free space ($= 8.854 \times 10^{-12}\,\mathrm{F\,m^{-1}}$), N the number density of the dipoles, μ the permanent dipole moment, k_B the Boltzmann constant ($= 1.381 \times 10^{-23}\,\mathrm{J\,K^{-1}}$) and g the Kirkwood correlation factor. The equation was recast to conform with SI units. The factor g is a measure of the short range order and is equal to 1 when no specific interactions between molecules occur. We applied this equation to our data, because the dielectric behavior of the orientationally-disordered solid is expected to resemble that of the polar liquid to a considerable extent. Since the temperature dependence of ϵ' is more Curie–Weiss-like than Curie-like for all the compounds, as shown in the figures, the term T was replaced by $(T - T_c)$ [10], where T_c is the Curie–Weiss temperature. For simplicity, no specific correlation between MA ions was assumed (therefore $g = 1$). The N values (5.47, 4.85 and $3.95 \times 10^{27}\,\mathrm{m^{-3}}$ for $MAPbCl_3$ $MAPbBr_3$ and $MAPbI_3$, respectively) were calculated from their molar volumes in the cubic phases reported by Poglitsch and Weber [3]. The ϵ' data measured at 100 kHz on cooling were used in the fitting, since these were not affected by the adsorbed water. Moreover, only the data which were deemed free from the influence of the transitions were used. As noted above, the cubic–tetragonal I transition caused no apparent change of the permittivity. However, good fits were not achieved if the experimental data for the fitting involved both the tetragonal I and cubic phases. Therefore, the best-fit function was determined separately. For $MAPbI_3$, only the tetragonal phase was analyzed in this way because the data set on the cubic phase was limited to a narrow temperature interval. A good fit was not achieved for the tetragonal phase of the $MAPbBr_3$, even though the general temperature dependence was similar for the three compounds. The results of the fitting are shown in Fig. 4. Parameters determined by the least-squares method are given in Table 2.

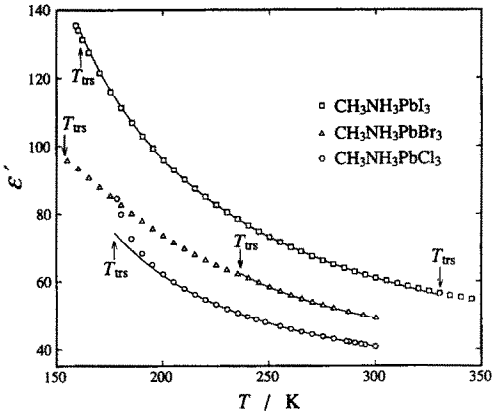

Fig. 4. Temperature dependence of the dielectric constant of the tetragonal (*I4/mcm*) phase and cubic phases of $CH_3NH_3PbX_3$ (X = Cl, Br, I) taken at 100 kHz. The best fit curves representing the modified Kirkwood–Fröhlich eqn (1) are shown as solid lines.

The dipole moment we obtained is $1.5–3.0 \times 10^{-30}\,\mathrm{C\,m}$. Comparable values were reported by Poglitsch and Weber [3]. According to an *ab initio* calculation of the electronic structure of the MA ion, the CH_3 group carries $+0.340e$ and NH_3 group $+0.660e$, where e is the positive elementary charge [11]. This may be regarded as $(0.5 - 0.160)e$ on CH_3 and $(0.5 + 0.160)e$ on NH_3, giving rise to a dipole moment of $0.160el = 3.98 \times 10^{-30}\,\mathrm{C\,m} = 1.193\mathrm{D}$, where $e = 1.602 \times 10^{-19}\,\mathrm{C}$ and $l = 0.1553\,\mathrm{nm}$, the C–N distance [11].

Table 2. Temperature regions of the dielectric constant data used in the fitting and optimized parameters in the modified Kirkwood–Fröhlich equation for $CH_3NH_3PbX_3$ (X = Cl, Br, I)

	$CH_3NH_3PbCl_3$	$CH_3NH_3PbBr_3$	$CH_3NH_3PbI_3$
Temperature region used in the fitting	210–300 K	250–300 K	180–300 K
Parameters optimized			
T_c (K)	96.9	123.4	78.4
μ (10^{-30} C m)	1.83	1.50	2.94
μ (D)	0.549	0.450	0.881
ϵ_∞	22.1	28.7	23.3

Tetragonal II *phase*

Both $MAPbCl_3$ and $MAPbBr_3$ have a tetragonal II phase over a narrow temperature range. Discontinuities of the dielectric constant occur at the tetragonal II–orthorhombic (I or II) transitions. The ϵ' values in this phase are much larger than those in the orthorhombic I or II phase. This indicates that a part of the dipoles are disordered (and hence respond to an applied electric field) in the tetragonal II phase. On the other hand, the increase of ϵ' with increasing temperature indicates that there is a long range order of the dipole moments in this phase [12]. These two observations are consistent with each other if one remembers that the long range order is not complete in the tetragonal II phase. In fact, the heat capacities of the tetragonal II phase of $MAPbBr_3$ and $MAPbCl_3$ are considerably larger than the normal vibrational heat capacity [4]. The excess heat capacities may be related to the disordering of this (partial) long range order.

In the previous paper [4], we interpreted the orientational disorder of the MA ion in this phase on the basis of the transition entropy. One model assumes that the MA ion is disordered over four equivalent orientations along the body diagonals of the tetragonal lattice but is ordered with respect to the C–N exchange and around the C–N axis. The other model is based upon the assumption that the MA ion is orientationally ordered along the tetragonal axis but is disordered with respect to the rotation about the C–N axis. The present experimental data showing a substantial orientational component in the permittivity in this phase are more in line with the first model, because one cannot expect an orientational dielectric response in the second model, in which the MA ions are disordered only about the C–N axis. However, the second model cannot be totally ruled out if one considers additional motion of the MA ion such as precession of the C–N axis about the tetragonal axis [6, 7], or partial disorder of the head-to-tail ordering. Some motion of the C–N axis was also supported by the ^2H NMR study in this phase [5].

Orthorhombic I *and* II *phases*

In these phases, the ϵ' values are practically temperature independent. Their magnitudes ($\epsilon' = 17$ for $MAPbCl_3$, 26 for $MAPbBr_3$, and 36 for $MAPbI_3$) are consistent with what one expects from electronic and ionic polarizations.

Weak dielectric dispersion and loss were found in $MAPbBr_3$ and $MAPbI_3$. Figures 5 and 6 show the real (upper) and imaginary (lower) parts of the dielectric permittivity for $MAPbBr_3$ and $MAPbI_3$, respectively. Symbols ○, △, □, ▽ and ◇ denote the data taken at frequencies of 100 Hz, 1 kHz, 10 kHz, 100 kHz and 1 MHz, respectively. The ϵ'' values at 100 Hz and 1 MHz contain a constant value of instrumental origin and thus should be shifted downward. As one can see in Figs 5 and 6, the dielectric dispersion and loss occurred in the same temperature range for the two compounds.

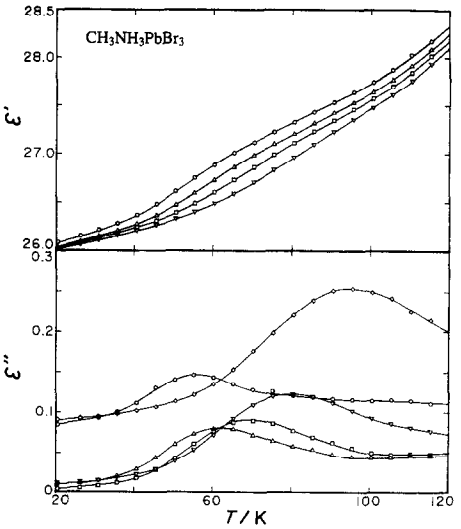

Fig. 5. Temperature dependence of the real (upper) and imaginary (lower) parts of the dielectric permittivity of $CH_3NH_3PbBr_3$ in the orthorhombic phase. ○: 100 Hz, △: 1 kHz, □: 10 kHz, ▽: 100 kHz, ◇: 1 MHz.

The temperatures at which the ϵ'' curves have a maximum at a particular frequency were read off from the figure. The relaxation time τ of the motion related to the dielectric dispersion was calculated by using the relation,

$$\tau = 1/(2\pi f). \tag{2}$$

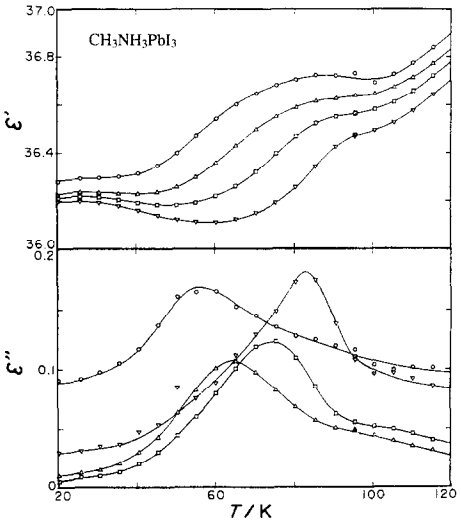

Fig. 6. Temperature dependence of the real (upper) and imaginary (lower) parts of the dielectric permittivity of $CH_3NH_3PbI_3$ in the orthorhombic phase. ○: 100 Hz, △: 1 kHz, □: 10 kHz, ▽: 100 kHz.

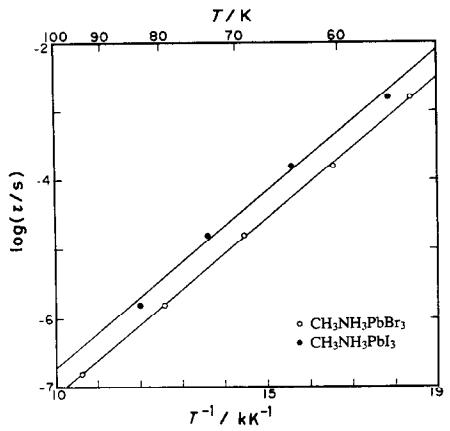

Fig. 7. Arrhenius plots of the dielectric relaxation time for $CH_3NH_3PbBr_3$ and $CH_3NH_3PbI_3$.

Figure 7 shows the Arrhenius plot of the relaxation time. The activation energies obtained from the plot are 9.8 and 9.7 kJ mol^{-1} for $MAPbBr_3$ and $MAPbI_3$, respectively.

We considered the MA ion to be ordered both with respect to the orientation of the C–N axis itself and around the C–N axis in the orthorhombic I or II phases on the basis of the experimental transition entropy [4]. It was therefore unexpected to find dielectric dispersions in $MAPbBr_3$ and $MAPbI_3$ in these phases. The temperatures at which the relaxation time becomes comparable to the calorimetric experimental time ($\sim 10^3$ s) are 33.7 K and 34.4 K for $MAPbBr_3$ and $MAPbI_3$, respectively. These temperatures were estimated by extrapolation of the Arrhenius plot. However, no glass transition was found at these temperatures in the heat capacity measurement. The orthorhombic II–tetragonal I (II for the bromide) transition is of the first order but there is a precursor effect below the transition temperature [see Figs 12 and 13 in Ref. 4]. The dielectric dispersion may be related to the partial disorder represented by the precursor effect. The magnitude of the dielectric dispersions is very small in comparison with the orientational effect at the orthorhombic II–tetragonal II (I for the iodide) transition. They are only about 1% and 0.5% for $MAPbBr_3$ and $MAPbI_3$, respectively. The activation energies 9.8 and 9.7 kJ mol^{-1} may represent the barriers which an MA ion experiences as it reorients in the crystal. However, the type of molecular motion responsible for the dispersion cannot be identified at present because of the small magnitude of the effect.

The results of our dielectric measurements on $MAPbX_3$ (X = Cl, R, I) can be summarized as follows: the MA ions are fully disordered in the cubic and tetragonal I phases. The dielectric constants in these phases are well described by the modified Kirkwood–Fröhlich equation. In the tetragonal II phase, the MA ions are partially disordered and further disordering of the molecular orientation proceeds with increasing temperature. The MA ions are completely ordered in the orthorhombic phases. A weak dielectric dispersion found in the orthorhombic II phase of the bromide and the iodide can be interpreted as a precursor effect of the phase transition from the orthorhombic II to tetragonal phase. The results obtained in the present study are consistent with the model proposed previously in a calorimetric study, involving MA ions which are disordered with respect to both the orientation of the C–N axis and the rotation around the C–N axis and undergo successive ordering at the respective transitions on cooling [4].

REFERENCES

1. Weber D., *Z. Naturforsch.* **33b,** 1443 (1978).
2. Wasylishen R. E., Knop O. and MacDonald J. B., *Solid State Commun.* **56,** 581 (1985).
3. Poglitsch A. and Weber D., *J. Chem. Phys.* **87,** 6373 (1987).
4. Onoda-Yamamuro N., Matsuo T. and Suga H., *J. Phys. Chem. Solids* **51,** 1383 (1990).
5. Knop O., Wasylishen R. E., White M. A., Cameron T. S. and Oort M. J. M. V., *Can. J. Chem.* **68,** 412 (1990).
6. Furukawa Y. and Nakamura D., *Z. Naturforsch.* **44a,** 1122 (1989).
7. Xu Q., Eguchi T., Nakayama H., Nakamura N. and Kishita M., *Z. Naturforsch.* **46a,** 240 (1991).
8. Matsuo T. and Suga H., *Solid State Commun.* **21,** 923 (1977).
9. Böttcher C. J. F., *Theory of Electric Polarization.* Scientific, Amsterdam (1973).
10. Böhmer R. and Loidl A., *J. Chem. Phys.* **89,** 4981 (1988).
11. Masamura M., *Chem. Phys. Lett.* **162,** 329 (1989).
12. Fröhlich H., *Theory of Dielectrics.* Oxford University Press, London (1958).